



# Bioelectrochemical enhancement of methane production from exhausted vine shoot fermentation broth by integration of MEC with anaerobic digestion

D. Carrillo-Peña<sup>1</sup> · A. Escapa<sup>1,2</sup> · M. Hijosa-Valsero<sup>3</sup> · A. I. Paniagua-García<sup>3</sup> · R. Díez-Antolínez<sup>3</sup> · R. Mateos<sup>1</sup>

Received: 16 March 2022 / Revised: 20 May 2022 / Accepted: 28 May 2022  
© The Author(s) 2022

## Abstract

A microbial electrolysis cell integrated in an anaerobic digestion system (MEC-AD) is an efficient configuration to produce methane from an exhausted vine shoot fermentation broth (EVS). The cell worked in a single-chamber two-electrode configuration at an applied potential of 1 V with a feeding ratio of 30/70 (30% EVS to 70% synthetic medium). In addition, an identical cell operated in an open circuit was used as a control reactor. Experimental results showed similar behavior in terms of carbon removal (70–76%), while the specific averaged methane production from cycle 7 was more stable and higher in the connected cell (MEC<sub>AD</sub>) compared with the unpolarized one (OC<sub>AD</sub>) accounting for  $403.7 \pm 33.6$  L CH<sub>4</sub>·kg VS<sup>-1</sup> and  $121.3 \pm 49.7$  L CH<sub>4</sub>·kg VS<sup>-1</sup>, respectively. In addition, electrochemical impedance spectroscopy revealed that the electrical capacitance of the bioanode in MEC<sub>AD</sub> was twice the capacitance shown by OC<sub>AD</sub>. The bacterial community in both cells was similar but a clear adaptation of *Methanosarcina* Archaea was exhibited in MEC<sub>AD</sub>, which could explain the increased yields in CH<sub>4</sub> production. In summary, the results reported here confirm the advantages of integrating MEC-AD for the treatment of real organic liquid waste instead of traditional AD treatment.

**Keywords** Anaerobic digestion · Electrochemical impedance spectroscopy · Methane enhancement · Microbial electrolysis cell · Vine shoot treatment

## 1 Introduction

Anaerobic digestion (AD) is a process in which microorganisms degrade high contents of organic matter from different types of waste (e.g., sewage sludge, food waste, animal manure, industrial and agricultural residues) by producing biogas via anaerobic metabolism [1–4]. The complexity of some raw materials requiring pre-treatment, and the

microbial processes involved, limits the metabolic development between species, leading to long hydraulic retention times (HRT), low efficiency in the bioconversion of organic waste to methane, and constant monitoring of parameters such as pH, temperature, feed flow rate, and inhibitors [5–7].

Microbial electrolysis cells (MEC) are a type of bioelectrochemical system capable of degrading organic matter and, depending on the cell configuration, producing hydrogen (H<sub>2</sub>) and/or methane (CH<sub>4</sub>) with the aid of a small energy input [8, 9]. Previous research by several authors has shown that the integration of a MEC-AD system can improve the overall performance of the system by showing (i) an increase in methane production yields; (ii) improved process stabilization; (iii) high organic matter removal; and (iv) conversion of hydrogen ions and volatile fatty acids into methane [10–19]. For instance, Moreno et al. [10] reported an improvement in the degradation of the organic matter contained in domestic wastewater by a MEC and an increase in the methane production rate versus a conventional AD. Hassanein et al. [12] improved productivity from 10.9 L CH<sub>4</sub> by AD to 23.6 L CH<sub>4</sub> via MEC in addition to increasing

✉ R. Mateos  
rmatg@unileon.es

<sup>1</sup> Chemical and Environmental Bioprocess Engineering Group, Natural Resources Institute (IRENA), Universidad de León, Avda. de Portugal 41, 24009 Leon, Spain

<sup>2</sup> Department of Electrical Engineering and Automatic Systems, Universidad de León, Campus de Vegazana s/n, 24071 León, Spain

<sup>3</sup> Centro de Innovación en Bioproductos Agroalimentarios (CIBAG), Instituto Tecnológico Agrario de Castilla Y León (ITACyL), Polígono Agroindustrial del Órbigo p.2-6, 24358 Villarejo de Órbigo, Spain

the chemical oxygen demand (COD) removal by applying a cell potential of 1 V. Finally, Zhao et al. [14] observed an increase in methane production from 23.8 to 45.6% in the MEC-AD reactor compared to the traditional one using acetate as a substrate. It has also been observed that the influence of using different types of wastes/compounds as substrates in MEC-AD systems could lead to a higher methane production yield compared against traditional AD [11, 16, 17, 19]. For example, Xu et al. [11] used brewery wastewater as a substrate increasing the methane yield by 30%, Prajapati and Singh [16] operated with unprocessed agriculture waste and achieved a twofold higher methane yield at 40 mV, Choi and Lee [19] treated food waste showing a maximum methane yield 1.2 times higher, and Wang et al. [17] used activated sludge waste exhibiting an increase in methane productivity between 9.5 and 7.8 times higher.

On the other hand, the production of bio-ethanol and bio-butanol from different sources is an important source of alternative fuels used for transport. In this way, vine shoot, which is a woody material generated during pruning activities in vineyards, represents the most important winery by-product in terms of volume. In the last few years, vine shoots have been used for butanol production via bacterial fermentation [20]. One of the existing methods to recover butanol from fermentation broths is gas stripping [21], through which a condensate fraction rich in butanol is separated from the broth. However, the remaining exhausted broth is left unused, constituting a liquid waste stream which should be correctly managed before its disposal.

Therefore, the objective of this study was to compare the treatment efficiency of MEC-AD and conventional AD for a real organic residue (exhausted vine shoot fermentation broth) from the final stream of a gas stripping process. More precisely, the investigation will focus on determining the effect of the electrodes and the applied voltage (1 V) to improve treatment performance (i.e., organic matter removal) and energy production ( $\text{CH}_4$ ). We also try to explain, by means of electrochemical impedance

spectroscopy, cyclic voltammetry, and microbiology analyses, the different behavior between the polarized and unpolarized electrodes.

## 2 Material and methods

### 2.1 MEC reactor setup

Two cells with a single-chamber configuration and a working volume of 0.5 L were used for the effluent treatment. The cells were equipped with connections for gas outlets and liquid inlets and outlets and contained the electrolytic module (anode + cathode) immersed in the feed material. The anode (working electrode) consisted of a carbon-felt piece (7 cm × 3 cm × 0.5 cm), and the cathode (counter electrode) was a stainless-steel piece (7 cm × 3 cm), both connected with titanium wire. The explanatory scheme was shown in Fig. 1. The first cell was operated as a MEC<sub>AD</sub> in a two-electrode configuration with an applied voltage of 1 V, using a Biologic multichannel potentiostat (software EC lab vs. 11.31). The second cell (OC<sub>AD</sub>) was operated in open circuit mode, keeping the same configuration as the previous one in order to know the endogenous production of the substrate. The cells were operated in batch mode at a constant temperature of  $25 \pm 2$  °C, and agitation speed of 300 rpm was fixed to enable mixing and facilitate mass transfer inside the chambers (magnetic stirrer plate IKA-WERKE RO 15, Germany).

### 2.2 Influent and growth media

The inoculum used in the present study was obtained from river sludge, and the used substrate is an exhausted vine shoot fermentation broth (EVS) [20]. The characterization of the influents is shown in Table 1. The EVS presents a high organic load evidenced by the total organic carbon (TOC) and a chemical oxygen demand (COD) around  $17 \pm 0.6$  g·L<sup>-1</sup>

**Fig. 1** Schematic representation of the laboratory set-up

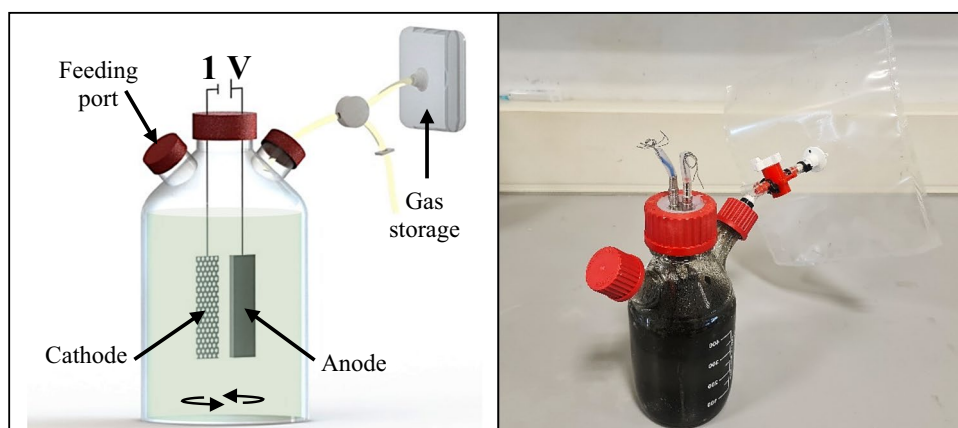


**Table 1** Characterization of inoculum and EVS used as influent in this study

Parameter	Units	Inoculum	Substrate
pH	-	7.1 ± 0.1	7.2 ± 0.1
Conductivity	mS·cm <sup>-1</sup>	-	18.2 ± 0.1
Redox	mV	-	71.0 ± 1.0
Total solids (TS)	g·kg <sup>-1</sup>	30.8 ± 0.9	55.5 ± 0.2
Volatile solids (VS)	g·kg <sup>-1</sup>	18.2 ± 0.5	25.3 ± 0.2
TOC	g·L <sup>-1</sup>	2.9 ± 0.2	17.2 ± 0.6
COD	g·L <sup>-1</sup>	2.2 ± 0.1	49.0 ± 1.0
Acetic	g·L <sup>-1</sup>	-	5.4 ± 0.1
Butyric	g·L <sup>-1</sup>	-	4.1 ± 0.1

and  $49 \pm 1$  g·L<sup>-1</sup>, respectively. This indicates that the EVS could be treated using anaerobic digestion/bioelectrochemical systems. The inoculation phase was carried out using 20% river sludge effluent, 30% EVS, and 50% synthetic medium (SM), and then the headspaces were flushed with N<sub>2</sub> gas for 30 min. The synthetic medium used contained the following: 1.07 g K<sub>2</sub>HPO<sub>4</sub>, 0.53 g KH<sub>2</sub>PO<sub>4</sub>, 0.15 g NH<sub>4</sub>Cl, 0.02 g CaCl<sub>2</sub>, 0.02 g MgSO<sub>4</sub>, 0.5 g NaCl, 0.1 g NaHCO<sub>3</sub> (pH 7.1), 1 mL of mineral solution, and 10 mL of vitamin solution per liter [22]. All solutions were filter sterilized and stored at 4 °C to prevent microbial growth. Distilled water was used for solution preparation, and the chemicals and reagents used were of analytical grade. In the origin, the substrate was subjected to gas stripping in order to recover and concentrate acetone, butanol, and ethanol in the condensate fraction [23]. The other fraction—containing the rest of the aqueous vine-shoot hydrolysate, nutrient leftovers, and cell debris—was named EVS, and it was assessed as a substrate in the AD-MEC experiments.

During the experimental phase of our study, the reactors were fed in batch (7 days duration) for 10 cycles. To prevent the occurrence of an organic shock due to the relatively high COD content of the EVS (Table 1), the feeding consisted of a mixture of 30/70 (v/v) EVS and SM. In addition, to ensure anaerobic conditions during the feed (start of every cycle), the cells were bubbled with nitrogen for 15 min. The amount of nitrogen present in the headspace at the start of each cycle remains inside the reactor and is deducted from the gas recovered at the end of the cycle.

### 2.3 Analytical and bioelectrochemical measurements

The analytical characterizations were performed at the end of each cycle. Gas composition was measured using a gas chromatograph (GC) (CTC Analytics model HXT Pal) equipped with a thermal conductivity detector (TCD) determining the gas composition in terms of H<sub>2</sub>, carbon dioxide

(CO<sub>2</sub>), oxygen (O<sub>2</sub>), nitrogen (N<sub>2</sub>), and CH<sub>4</sub>. Volatile fatty acids (VFAs) were analyzed using a GC (Bruker 450-GC) with a flame ionization detector (FID). Total organic carbon (TOC), total inorganic carbon (IC), and total nitrogen (TN) were measured in an analyzer (multi N/C 3100, Analytik Jena). Dissolved oxygen (Hach, HQ40d—two-channel digit multimeter), redox (pH-Meter, pH 91; Wissenschaftlich Technische Werkstätten, WTW), and pH (pH-Meter BASIC 20+, Crison) measurements were performed following standard methodologies.

Bioelectrochemical characterizations were also carried out at the beginning and end of the experiment to qualitatively distinguish between the biotic and abiotic performances of the system in a three-electrode configuration using an Ag/AgCl (3 M) electrode as a reference. Cyclic voltammeteries (CV) from 0.2 to -0.6 V were performed imposing a linear scanning potential rate of 5 mV·s<sup>-1</sup>, and electrochemical impedance spectroscopy (EIS) was carried out in a frequency range of 10<sup>5</sup>–10<sup>-2</sup> Hz. The EIS data were fitted to an equivalent electrical circuit with the help of the EC-lab® software version 11.31. The electrical circuit that best matched the characteristics of the Nyquist diagram for each electrode was selected.

### 2.4 Extraction of DNA and microbial community structure determination

Approximately 5 cm<sup>2</sup> of surface area (one tenth of the electrode), which is around 300 mg of sample, was extracted from the electrode-biofilms, and, for the bulk, about 50 mL of sample was taken and centrifuged to extract about 300 mg of sediment in MEC<sub>AD</sub> and OC<sub>AD</sub> cells. Those samples were used to characterize the microbial communities that had developed in the bioanodes and the bulk at the end of the experiment (cycle 10). Microbial communities were analyzed and followed along the experimental time by high throughput sequencing of massive 16S rRNA gene libraries. Total Bacteria and Archaea were analyzed. Genomic DNA was extracted with a DNeasy PowerSoil kit (Qiagen) according to manufacturer's instructions. All polymerase chain reaction (PCR) were carried out in a Mastercycler (Eppendorf, Hamburg, Germany), and PCR samples were checked for size of the product on a 1% agarose gel and quantified by NanoDrop 1000 (Thermo Scientific). The entire DNA extract was used for high-throughput sequencing of 16S rRNA gene-based massive libraries with 16S rRNA gene-based primers for Bacteria 27Fmod-519R and for Archaea 349F-806R. The Novogene Company (Cambridge, UK) carried out Illumina sequencing using a HiSeq 2500 PE250 platform.

The obtained DNA reads were compiled in FASTq files for further bioinformatics processing carried out using QIIME software version 1.7.0 [24]. Sequence analyses

were performed by Uparse software (version 7.0.1001) using all of the effective tags. Sequences with  $\geq 97\%$  similarity were assigned to the same operative taxonomic units (OTUs). Representative sequences for each OTU was screened for further annotation. For each representative sequence, Mothur software was performed against the SSUrRNA database of the SILVA Database [25] for species annotation at each taxonomic rank (Threshold: 0.8–1).

The quantitative analysis of all samples was analyzed by means of quantitative-PCR reaction (qPCR) using PowerUp SYBR Green Master Mix (Applied Biosystems) in a StepOnePlus Real-Time PCR System (Applied Biosystems). The qPCR amplification was performed for the 16S rRNA gene in order to quantify the entire eubacteria community and for the *mcrA* gene to quantify the total methanogen community. The primer set 314F qPCR (5'-CCTACGGGAGGCAGCAG-3') and 518R qPCR (5'-ATTACCGCGGCTGCTGG-3') at an annealing temperature of 60 °C for 30 s was used for Bacteria and Archaea 349F (5'-GYGCASCAGKCGMGAAW-3') and Arc 806R (5'-GGACTACVSGGGTATCTAAT-3') for Archaea quantification.

### 3 Results and discussion

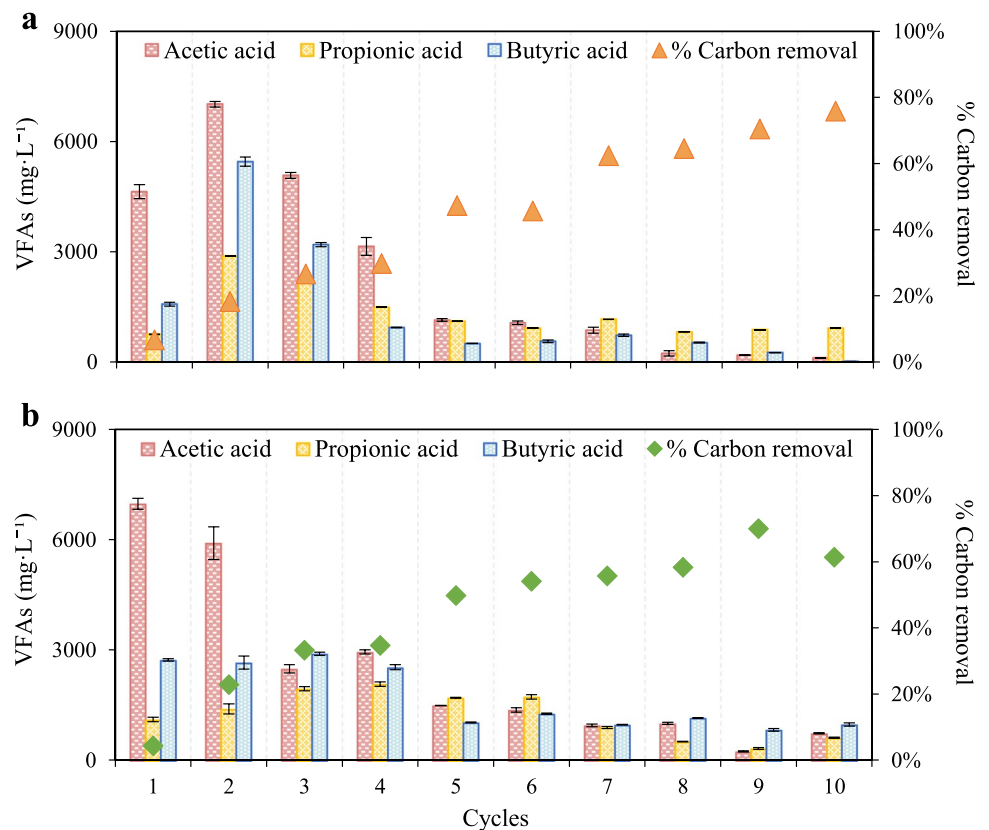
#### 3.1 Carbon removal and gas recovery of the cells

Current density, which is indicative of the activity of electrogenic bacteria, in the cell operated with an applied voltage  $MEC_{AD}$  started to increase right after inoculation. After three consecutive cycles, the current profiles began to be repeatable (supplementary information; Fig. S1). At that point,  $MEC_{AD}$  and  $OC_{AD}$  started to be fed in batch mode (7 days duration) with the diluted exhausted vine shoot fermentation broth (DEVS).

TOC removal showed a similar trend in both cells, increasing steadily as the cycles go by, which reveals an adaptation process of the microbial communities. Results also indicate that TOC removal in  $OC_{AD}$  tends to stabilize at about 60%, while in  $MEC_{AD}$ , there seems to be a slight growing trend achieving removal rates of about 75%. This is coherent with the evolution of the concentration of VFAs (acetic and butyric acids) at the end of the cycles, where  $MEC_{AD}$  manages to remove all the acetic and butyric acids, while a significant amount of VFAs remains in  $OC_{AD}$  at the end of the cycle (Fig. 2).

The differences in performance between  $MEC_{AD}$  and  $OC_{AD}$  became more prominent when considering gas

**Fig. 2** VFA evolution in terms of acetic, propionic, and butyric acid concentration and carbon removal percentage for **a**  $MEC_{AD}$  and **b**  $OC_{AD}$  cells



production and composition (Fig. 3). Indeed, methane concentration in the off-gas and the specific methane production were consistently higher in MEC<sub>AD</sub> from the beginning. From cycle 3 onwards, the averaged methane composition was 60% ± 4% in OC<sub>AD</sub> (comparable to the typical values found in anaerobic digestion with this type of substrates [26]) and 71% ± 6% in MEC<sub>AD</sub>. Similar results can be found in the literature with a methane content in the gas phase typically between 55 and 65% [27]. In addition, while specific methane production in MEC<sub>AD</sub> grew steadily and tended to stabilize at around 403.7 ± 33.6 L CH<sub>4</sub>·kg VS<sup>-1</sup> from cycle 7 onwards, it became more erratic and much lower in OC<sub>AD</sub>, averaging 121.3 ± 49.7 L CH<sub>4</sub>·kg VS<sup>-1</sup> but dropping to 83.7 L CH<sub>4</sub>·kg VS<sup>-1</sup> in cycle 10.

In summary, the main advantage of a MEC<sub>AD</sub> system with an applied voltage of 1 V is its higher carbon transformation capacity and better VFA utilization, resulting in an increased methane production rate (approximately 61% more biogas and 69% more CH<sub>4</sub> compared to a normal digestion), which agrees with previously reported results [13, 14, 28].

### 3.2 Bioelectrochemical characterizations

EIS and CV analyses were done at the end of cycle 10 to gain insight in the properties of the anodic biofilms of MEC<sub>AD</sub> and OC<sub>AD</sub> (an abiotic carbon felt electrode was also used as a control). The OC<sub>AD</sub> shows an incipient electrochemical activity on the oxidative region of the voltammogram, which indicates that even in the absence of an applied voltage during cultivation, an electroactive biofilm develops on the surface of the anode (Fig. 4a). Aside from that, there is little difference between OC<sub>AD</sub> and the abiotic electrode. In contrast, the voltammogram of MEC<sub>AD</sub> shows two well-developed catalytic waves (oxidative and reductive waves at the edges of the MEC<sub>AD</sub>), which is indicative of a fully electroactive biofilm. Moreover, its width is significantly larger than OC<sub>AD</sub>, which indicates the existence of a larger capacitance and/or pseudo-capacitance in the MEC<sub>AD</sub> as seen below, in accordance with the results of other authors [29, 30].

The cells were subjected to EIS analysis to better understand their electrochemical performance. It is common to analyze EIS data by fitting them to a mathematical model of an electrical equivalent circuit (EEC), whose overall electrical impedance describes the electrochemical processes of the

**Fig. 3** MEC<sub>AD</sub> and OC<sub>AD</sub> cells evolution along cycles in terms of **a** biogas composition and **b** specific biomethane production (BM)

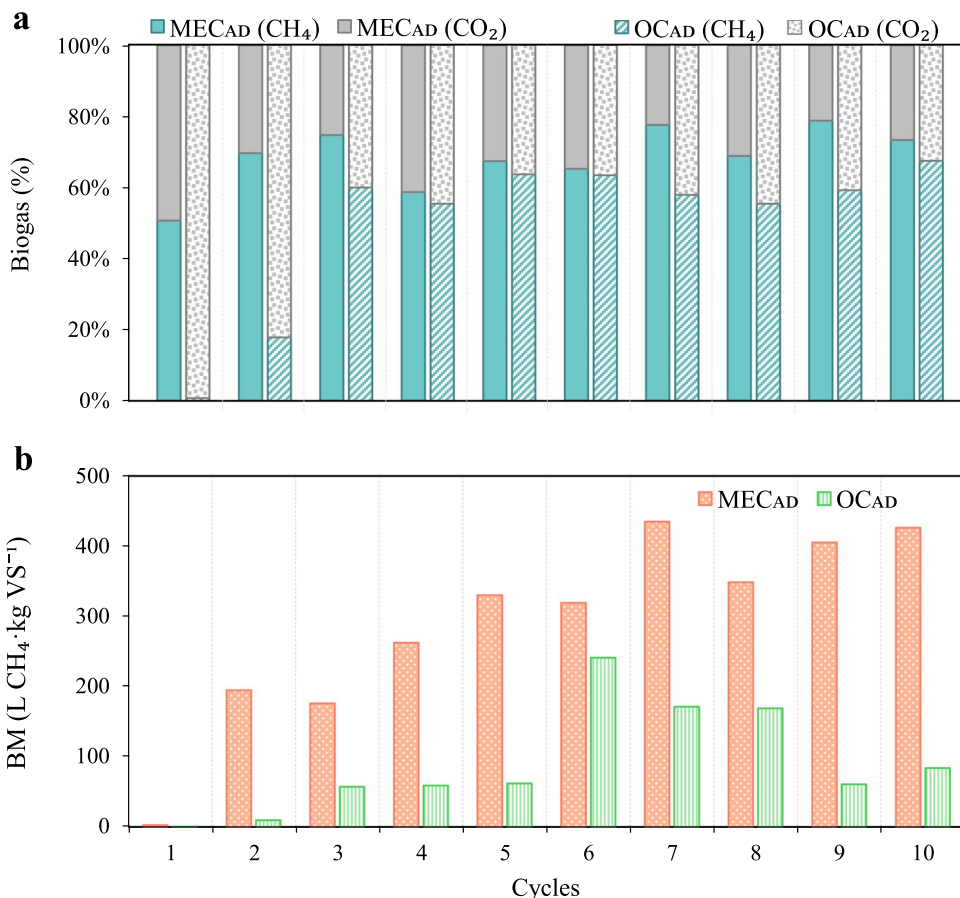
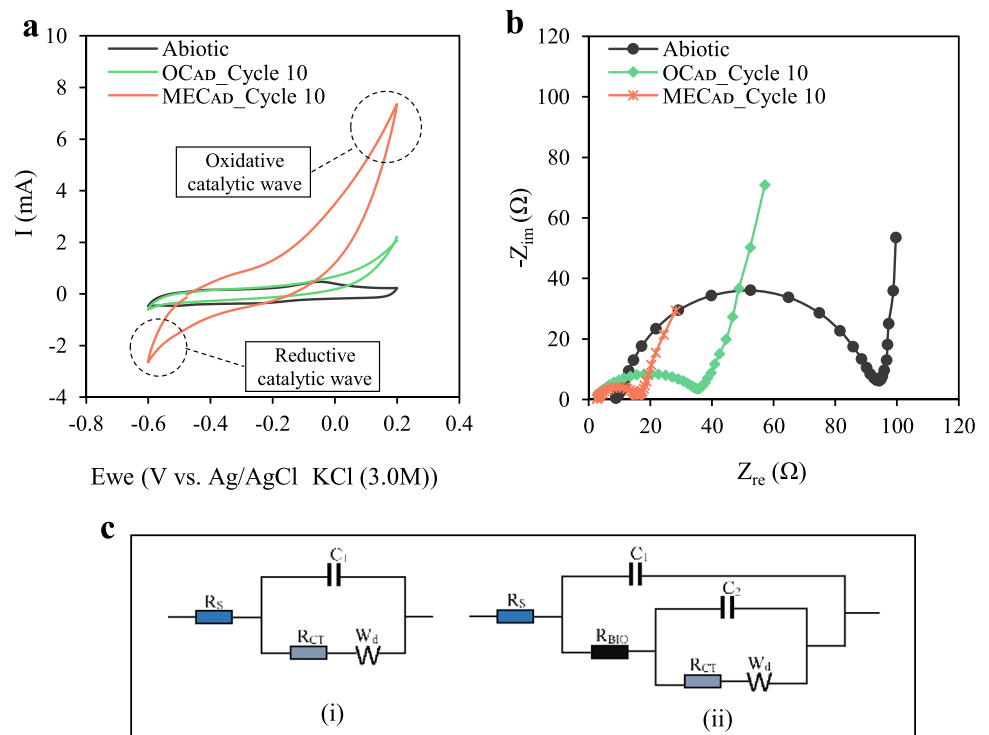


**Fig. 4** **a** Cyclic voltammetry and **b** electrochemical impedance spectroscopy using a Nyquist plot for the abiotic, MEC<sub>AD</sub>, and OC<sub>AD</sub> electrodes. **c** Electrical circuit used to fit EIS data for abiotic, MEC<sub>AD</sub>, and OC<sub>AD</sub> electrodes



system evaluated [31]. In this study, the EEC that best fits the Nyquist data in Fig. 4c was selected with aid of the EC lab software version 11.31. For the abiotic electrode (Fig. 4c, left), the EEC that best fits the data consists of (i)  $R_S$ , an ohmic resistance component that comprises the sum of the electrode resistance, the electrolyte solution resistance, and the contact resistance between the electrode and the current collector; (ii)  $R_{CT}$ , an electrochemical charge transfer resistance, related to charge transfer reactions; (iii)  $C_1$ , a capacitor that accounts for the capacitance of the electric double layer (charge accumulation at the interface of the electrode and the solution); and (iv)  $W_d$ , a Warburg's diffusion element related to the diffusion of reacting species in the vicinity of the electrode. For the two bioanodes (MEC<sub>AD</sub> and OC<sub>AD</sub>), the EEC that best fits the Nyquist data differs significantly (Fig. 4c, right). In addition to the elements described for the abiotic electrode, it includes (i)  $R_{BIO}$ , which according to [32] models both the charge transfer resistance between the electrode and the biofilm and the transport resistance of electrons in the biofilm; and (ii)  $C_2$ , an extra capacitance that represents the biofilm capacitance. The EIS data fitting results for the three anodes (Abiotic, OC<sub>AD</sub> and MEC<sub>AD</sub>) are shown in Table 2.

The  $R_{CT}$ , given by the diameter of the semicircle in the Nyquist plot, is more than 11 times lower in the MEC<sub>AD</sub> electrode compared to the abiotic electrode, indicating that charge transfer is greatly enhanced by the presence of an electroactive biofilm. This same parameter for the OC<sub>AD</sub>

**Table 2** EIS fitting data for abiotic, OC<sub>AD</sub>, and MEC<sub>AD</sub> electrodes in cycle 10

Parameter	Abiotic	OC <sub>AD</sub>	MEC <sub>AD</sub>
$R_S$	9.7 $\Omega$	3.3 $\Omega$	2.8 $\Omega$
$R_{CT}$	75.3 $\Omega$	16.3 $\Omega$	6.7 $\Omega$
$R_{BIO}$	-	11.4 $\Omega$	4.7 $\Omega$
$C_1$	14.0 $\mu\text{F}$	11.7 $\mu\text{F}$	32.0 $\mu\text{F}$
$C_2$	-	1.4 $\mu\text{F}$	6.0 $\mu\text{F}$

electrode is also relatively low (although more than twice higher than in MEC<sub>AD</sub>), which suggests that an incipient electroactive biofilm was developing on this electrode too, in spite of not being polarized. It seems that the biofilm also plays a significant role in facilitating electrical conductivity similar to behavior observed by other authors [33].  $R_{BIO}$  was about 2.5 times lower in MEC<sub>AD</sub> which indicates that the polarization of the electrode during its cultivation has a positive effect on the electrical conductivity of the anodic biofilm.

The electrical capacitance ( $C_1$  and  $C_2$ ) was significantly higher in MEC<sub>AD</sub>, indicating that the capacitance that arises due to electrostatic charge accumulation and/or the pseudocapacitance, which emerges from fast surface redox reactions, is caused by electroactive microorganisms [34]. This result is coherent with higher capacitance already observed in the CV analyses (Fig. 4a).

### 3.3 Microbiological characterization of the electrodes and bulks of MECs

Figure 5 shows the quantifications (qPCR) of Bacteria and Archaea populations on the biofilms and bulks of the MEC<sub>AD</sub> and OC<sub>AD</sub> cells in terms of the gene copy numbers. Both cells were dominated by a diverse group of Bacteria and to a lesser extent by Archaea. MEC<sub>AD</sub> has the highest microbiological activity centered on the electrode with 31% and 77% more Bacteria and Archaea than the bulk, respectively. This could be attributed to the fact that an applied voltage accelerated the transference of electrons between species, which further improved the microbial growth on the electrode surface [35, 36]. In contrast, the unconnected cell has the highest biomass growth in the bulk with 62% more Bacteria with respect to the electrode. Knowing that both cells remove the same amount of carbon but do not produce the same amount of methane, it could be assumed that the organic matter in the OC<sub>AD</sub> cell is being transformed into biomass that remains in the bulk. The above statement could be confirmed by the carbon balance of each cell (supplementary information; Fig. S2b), which shows the amount of organic carbon converted into biomass during each cycle. Higher organic carbon was observed for OC<sub>AD</sub> in the last three cycle (57–65%) compared to MEC<sub>AD</sub>, which explains the greater amount of gene copy number found in OC<sub>AD</sub> electrode.

The microbial community structure at genus level, in terms of Bacteria and Archaea, for electrodes and bulks of the cells under stable conditions were characterized by high throughput 16S rDNA amplicon sequencing gene. Concentrations of microorganisms less than 1% were categorized as “others.” No significant differences in microbial diversity in terms of Bacteria were observed between samples (Fig. 6a), while in terms of Archaea, a clear difference in communities was observed (Fig. 6b) between the cell working under an applied potential (MEC<sub>AD</sub>) and the

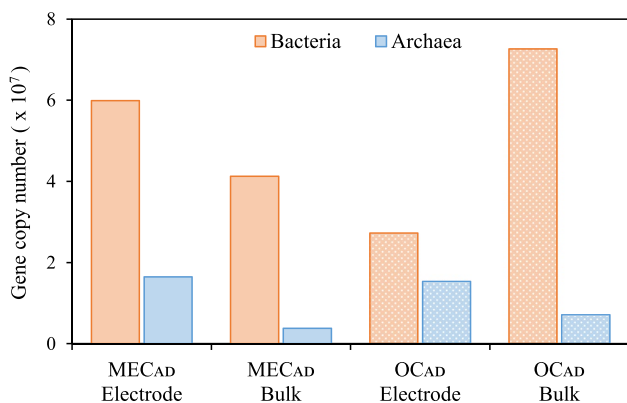


**Fig. 5** Total gene copy number in MEC<sub>AD</sub> and OC<sub>AD</sub> electrodes and bulks in terms of Bacteria and Archaea

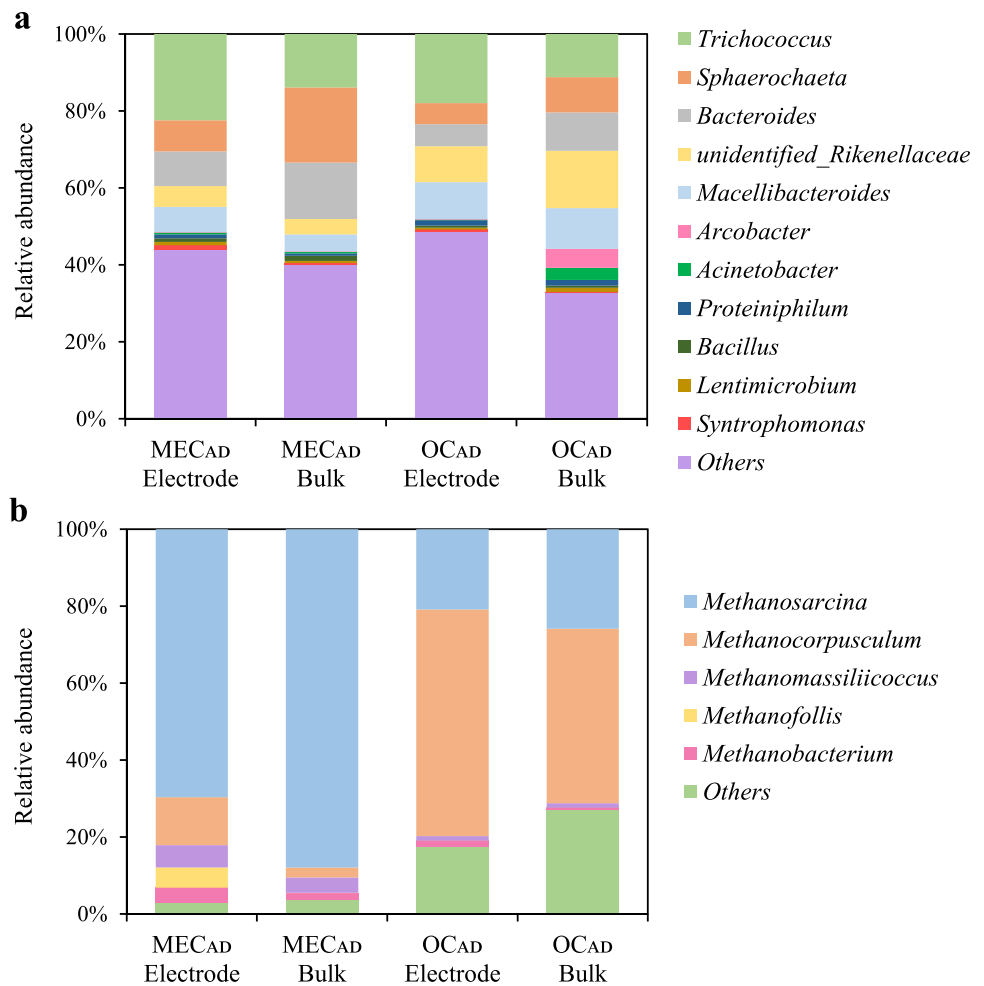
one operated in an open circuit (OC<sub>AD</sub>). These facts demonstrate that an applied voltage can promote the functional enrichment of microorganisms on the electrode and bulk, which improves process stability and methane production [31].

Firmicutes, Bacteroidetes, Proteobacteria, and Spirochaetes were the main families that dominated the four samples with and without an applied voltage (supplementary information; Fig. S3). The *Trichococcus* genus was the most abundant bacteria present in all samples (11–22%) being able to produce VFAs, such as acetate and lactate [37]. In addition, the *Macellibacteroides* and *Bacteroides* genus were also found and are the main VFA-producing bacteria present in the fermentative processes that use proteins or amino acids as substrates [38]. The *Bacteroides* genus is an exoelectrogenic bacteria mainly involved in the degradation of complex compounds to produce acetate commonly found in electrochemical systems [39, 40] and propionic acid [41]. Another possible exoelectrogenic fermenting bacteria in the system is the genus *Sphaerochaeta*, which is a hydrogen producer [42]. However, it can be considered that methane is also being produced by the acetoclastic pathway in which fermentative products (VFAs) carried out by bacteria are taken as substrate.

Figure 6b shows the dominant methanogens in MEC<sub>AD</sub> and OC<sub>AD</sub> cells for the electrodes and bulks. MEC<sub>AD</sub> operated with an applied voltage was dominated by *Methanosarcina* (70–88%) and to a lesser extent by the *Methanocorpusculum* genus. *Methanosarcina* can degrade various types of substrates, including propionate [43], acetate, H<sub>2</sub>, and CO<sub>2</sub> to be used in methanogenesis, resulting in high biogas production [42, 44]. *Methanosarcina* could be displacing *Methanocorpusculum* in the MEC<sub>AD</sub> reactor due to its versatility, taking advantage of both VFAs and hydrogen for methane production. It also has been found by Saif et al. [44] that *Methanosarcina*, together with Bacteria *Sphaerochaeta*, are involved in methane production. This summarizes that the connected cell has greater versatility in having microorganisms that carry out methanogenesis by both hydrogenotrophic and acetoclastic routes. Thus, it can be hypothesized that the high relative abundance of *Methanosarcina* in MEC<sub>AD</sub> would explain the increased methane production in the reactor if it is assumed that hydrogen is being produced on the cathode.

Nevertheless, the unpolarized cell (OC<sub>AD</sub>) had a relatively high abundance of *Methanocorpusculum* (45–59%) and a lower proportion of *Methanosarcina* (21–26%). *Methanocorpusculum* is a strictly hydrogenotrophic methanogen capable of producing methane from CO<sub>2</sub> in the presence of H<sub>2</sub> as an electron donor [45]. This same type of methanogenic Archaea is characteristic of systems treated by anaerobic digestion [46]. The above implies that the main methane production route used by the open-circuit cell

**Fig. 6** Taxonomic classification of 16S rDNA amplicon sequencing gene from **a** Bacteria and **b** Archaea at the genus level for the electrodes and bulks of MEC<sub>AD</sub> and OC<sub>AD</sub> cells



is hydrogenotrophic and explains the greater difficulty in degrading acetate in OC<sub>AD</sub>.

## 4 Conclusion

This work tries to assess the capability of MEC to valorize organic wastes generated from vine shoots and promote the enhancement of biogas production with respect to an open-circuit cell. The cell polarized at 1 V (MEC<sub>AD</sub>) present a similar percentage of carbon removal compared with the unpolarized cell (OC<sub>AD</sub>). Regarding the utilization of the carbon removed, MEC<sub>AD</sub> was found to have a greater capacity to transform carbon into a product of greater benefit (CH<sub>4</sub>) and, in addition, achieves better biogas quality from the start-up of the study. Working with an applied voltage may result in cells with higher electrochemical activity and conductivity and lower resistance to charge transfer, which may lead to better interactions between the microorganisms and the electrode. Moreover, CV and EIS analysis showed a higher capacitance for MEC<sub>AD</sub> due to the presence of electroactive microorganisms.

Bacterial microbial communities in both electrodes and cell bulks were very similar. However, there were notable differences in the methanogenic communities in the cells. OC<sub>AD</sub> was relatively dominated by the genus *Methanocorpusculum*, so the methanogenic pathway was strictly promoted by hydrogenotrophic microorganisms, which could have influenced the low biogas production. Moreover, MEC<sub>AD</sub> was dominated mostly by the genus *Methanosarcina* so the methanogenic process was promoted by the acetoclastic and hydrogenotrophic pathway, which could lead to better carbon utilization and high biogas production. It is possible to highlight the potential of microbial electrolysis cells compared to conventional anaerobic digestion in which the treatment and utilization of an exhausted vine shoot fermentation broth is improved.

**Supplementary Information** The online version contains supplementary material available at <https://doi.org/10.1007/s13399-022-02890-7>.

**Author contribution** Conceptualization: D. Carrillo-Peña, A. Escapa, R. Díez-Antolínez, R. Mateos. Methodology: D. Carrillo-Peña, M. Hijosa-Valsero, A.I. Paniagua-García. Formal analysis and investigation: D. Carrillo-Peña, M. Hijosa-Valsero, A.I. Paniagua-García.



Writing, original draft preparation: D. Carrillo-Peña, M. Hijosa-Valsero. Writing, review and editing: A. Escapa, R. Mateos. Funding acquisition: A. Escapa, R. Díez-Antolínez, R. Mateos. Supervision: A. Escapa, R. Díez-Antolínez, R. Mateos.

**Funding** Open Access funding provided thanks to the CRUE-CSIC agreement with Springer Nature. This work was financial supported by the European Regional Development Fund (FEDER) and Interreg V-A España-Portugal (POCTEP) 2014–2020 through the project: “Desarrollo de una estrategia transfronteriza para la valorización ecosostenible de biomásas residuales del sector vinícola y vitivinícola en Biorrefinerías integrales para la producción de Biocombustibles y Bioproductos” (BIOVINO) [0688\_BIOVINO\_6\_EJ].

## Declarations

**Conflict of interest** The authors declare no competing interests.

**Open Access** This article is licensed under a Creative Commons Attribution 4.0 International License, which permits use, sharing, adaptation, distribution and reproduction in any medium or format, as long as you give appropriate credit to the original author(s) and the source, provide a link to the Creative Commons licence, and indicate if changes were made. The images or other third party material in this article are included in the article's Creative Commons licence, unless indicated otherwise in a credit line to the material. If material is not included in the article's Creative Commons licence and your intended use is not permitted by statutory regulation or exceeds the permitted use, you will need to obtain permission directly from the copyright holder. To view a copy of this licence, visit <http://creativecommons.org/licenses/by/4.0/>.

## References

- Rasapoor M, Young B, Brar R et al (2020) Recognizing the challenges of anaerobic digestion: critical steps toward improving biogas generation. *Fuel* 261:116497. <https://doi.org/10.1016/J.FUEL.2019.116497>
- Van DP, Fujiwara T, Tho BL et al (2020) A review of anaerobic digestion systems for biodegradable waste: configurations, operating parameters, and current trends. *Environ Eng Res* 25:1–17. <https://doi.org/10.4491/EER.2018.334>
- González R, Blanco D, Cascallana JG et al (2021) Anaerobic co-digestion of sheep manure and waste from a potato processing factory: techno-economic analysis. *Fermentation* 7:235. <https://doi.org/10.3390/FERMENTATION7040235>
- Jaimes-Estévez J, Castro L, Escalante H, et al (2020) Cheese whey co-digestion treatment in a tubular system: microbiological behaviour along the axial axis. *Biomass Convers Biorefinery* 1–10. <https://doi.org/10.1007/S13399-020-00988-4/FIGURES/6>
- Khanal SK (2009) Bioenergy generation from residues of biofuel industries. In: *Anaerobic biotechnology for bioenergy production: Principles and Applications*. John Wiley & Sons, Ltd, pp 161–188
- Náthia-Neves G, Berni M, Dragone G et al (2018) Anaerobic digestion process: technological aspects and recent developments. *Int J Environ Sci Technol* 15:2033–2046. <https://doi.org/10.1007/S13762-018-1682-2/TABLES/3>
- Dey R, Maarisetty D, Baral SS (2022) A comparative study of bioelectrochemical systems with established anaerobic/aerobic processes. *Biomass Convers Biorefinery* 2021 1:1–16. <https://doi.org/10.1007/S13399-021-02258-3>
- Escapa A, Gil-Carrera L, García V, Morán A (2012) Performance of a continuous flow microbial electrolysis cell (MEC) fed with domestic wastewater. *Biores Technol* 117:55–62. <https://doi.org/10.1016/J.BIORTECH.2012.04.060>
- San-Martín MI, Leicester DD, Heidrich ES et al (2018) Bioelectrochemical systems for energy valorization of waste streams. In: *Energy Systems and Environment*. IntechOpen, pp 127–1142
- Moreno R, San-Martín MI, Escapa A, Morán A (2016) Domestic wastewater treatment in parallel with methane production in a microbial electrolysis cell. *Renewable Energy* 93:442–448. <https://doi.org/10.1016/J.RENENE.2016.02.083>
- Xu S, Zhang Y, Luo L, Liu H (2019) Startup performance of microbial electrolysis cell assisted anaerobic digester (MEC-AD) with pre-acclimated activated carbon. *Bioresour Technol Rep* 5:91–98. <https://doi.org/10.1016/J.BITEB.2018.12.007>
- Hassanein A, Witarsa F, Lansing S et al (2020) Bio-electrochemical enhancement of hydrogen and methane production in a combined anaerobic digester (AD) and microbial electrolysis cell (MEC) from dairy manure. *Sustainability (Switzerland)* 12:1–12. <https://doi.org/10.3390/su12208491>
- Zhao Z, Zhang Y, Ma W et al (2016) Enriching functional microbes with electrode to accelerate the decomposition of complex substrates during anaerobic digestion of municipal sludge. *Biochem Eng J* 111:1–9. <https://doi.org/10.1016/J.BEJ.2016.03.002>
- Zhao L, Wang XT, Chen KY et al (2021) The underlying mechanism of enhanced methane production using microbial electrolysis cell assisted anaerobic digestion (MEC-AD) of proteins. *Water Res* 201:117325. <https://doi.org/10.1016/J.WATRES.2021.117325>
- Arenas Sevillano CB, Chiappero M, Gomez X et al (2020) Improving the anaerobic digestion of wine-industry liquid wastes: treatment by electro-oxidation and use of biochar as an additive. *Energies* 13:5971. <https://doi.org/10.3390/EN13225971>
- Prajapati KB, Singh R (2020) Enhancement of biogas production in bio-electrochemical digester from agricultural waste mixed with wastewater. *Renewable Energy* 146:460–468. <https://doi.org/10.1016/J.RENENE.2019.06.154>
- Wang XT, Zhao L, Chen C et al (2021) Microbial electrolysis cells (MEC) accelerated methane production from the enhanced hydrolysis and acidogenesis of raw waste activated sludge. *Chem Eng J* 413:127472. <https://doi.org/10.1016/J.CEJ.2020.127472>
- Quashie FK, Fang A, Wei L, et al (2021) Prediction of biogas production from food waste in a continuous stirred microbial electrolysis cell (CSMEC) with backpropagation artificial neural network. *Biomass Convers Biorefinery* 1–12. <https://doi.org/10.1007/S13399-020-01179-X/FIGURES/7>
- Choi JM, Lee CY (2019) Bioelectrochemical enhancement of methane production in anaerobic digestion of food waste. *Int J Hydrogen Energy* 44:2081–2090. <https://doi.org/10.1016/J.IJHYDENE.2018.08.153>
- Garita-Cambronero J, Paniagua-García AI, Hijosa-Valsero M, Díez-Antolínez R (2021) Biobutanol production from pruned vine shoots. *Renewable Energy* 177:124–133. <https://doi.org/10.1016/J.RENENE.2021.05.093>
- Hijosa-Valsero M, Garita-Cambronero J, Paniagua-García AI, Díez-Antolínez R (2020) A global approach to obtain biobutanol from corn stover. *Renewable Energy* 148:223–233. <https://doi.org/10.1016/J.RENENE.2019.12.026>
- Bajracharya S, ter Heijne A, Dominguez Benetton X et al (2015) Carbon dioxide reduction by mixed and pure cultures in microbial electrosynthesis using an assembly of graphite felt and stainless steel as a cathode. *Biores Technol* 195:14–24. <https://doi.org/10.1016/J.BIORTECH.2015.05.081>
- Díez-Antolínez R, Hijosa-Valsero M, Paniagua-García AI, Gómez X (2018) In situ two-stage gas stripping for the recovery of butanol from acetone-butanol-ethanol (ABE) fermentation broths. *Chem Eng Trans* 64:37–42. <https://doi.org/10.3303/CET1864007>

24. Caporaso JG, Kuczynski J, Stombaugh J et al (2010) QIIME allows analysis of high-throughput community sequencing data. *Nat Methods* 7:335–336. <https://doi.org/10.1038/nmeth.f.303>
25. Wang Q, Garrity GM, Tiedje JM, Cole JR (2007) Naïve Bayesian classifier for rapid assignment of rRNA sequences into the new bacterial taxonomy. *Appl Environ Microbiol* 73:5261–5267. <https://doi.org/10.1128/AEM.00062-07>
26. Da Ros C, Cavinato C, Bolzonella D, Pavan P (2016) Renewable energy from thermophilic anaerobic digestion of winery residue: preliminary evidence from batch and continuous lab-scale trials. *Biomass Bioenerg* 91:150–159. <https://doi.org/10.1016/J.BIOMBIOE.2016.05.017>
27. Angelidaki I, Karakashev D, Batstone DJ, et al (2011) Biomethanation and its potential. In: *Methods in Enzymology*. Academic Press Inc., pp 327–351
28. Alonso RM, Escapa A, Sotres A, Morán A (2020) Integrating microbial electrochemical technologies with anaerobic digestion to accelerate propionate degradation. *Fuel* 267:. <https://doi.org/10.1016/j.fuel.2020.117158>
29. Carmona-Martínez AA, Lacroix R, Trably E et al (2018) On the actual anode area that contributes to the current density produced by electroactive biofilms. *Electrochim Acta* 259:395–401. <https://doi.org/10.1016/J.ELECTACTA.2017.10.200>
30. Venkata Mohan S, Veer Raghavulu S, Sarma PN (2008) Influence of anodic biofilm growth on bioelectricity production in single chambered mediatorless microbial fuel cell using mixed anaerobic consortia. *Biosens Bioelectron* 24:41–47. <https://doi.org/10.1016/J.BIOS.2008.03.010>
31. Kretzschmar J, Harnisch F (2021) Electrochemical impedance spectroscopy on biofilm electrodes – conclusive or euphonious? *Curr Opin Electrochem* 29:100757. <https://doi.org/10.1016/J.COIELEC.2021.100757>
32. ter Heijne A, Liu D, Sulonen M et al (2018) Quantification of bioanode capacitance in bioelectrochemical systems using electrochemical impedance spectroscopy. *J Power Sources* 400:533–538. <https://doi.org/10.1016/J.JPOWSOUR.2018.08.003>
33. Cai W, Zhang Z, Ren G et al (2016) Quorum sensing alters the microbial community of electrode-respiring bacteria and hydrogen scavengers toward improving hydrogen yield in microbial electrolysis cells. *Appl Energy* 183:1133–1141. <https://doi.org/10.1016/J.APENERGY.2016.09.074>
34. Malvankar NS, Mester T, Tuominen MT, Lovley DR (2012) Supercapacitors based on c-type cytochromes using conductive nanostructured networks of living bacteria. *ChemPhysChem* 13:463–468. <https://doi.org/10.1002/CPHC.201100865>
35. Guo H, Hua J, Cheng J et al (2022) Microbial electrochemistry enhanced electron transfer in lactic acid anaerobic digestion for methane production. *J Clean Prod* 358:131983. <https://doi.org/10.1016/J.JCLEPRO.2022.131983>
36. Li Y, Chen Y, Wu J (2019) Enhancement of methane production in anaerobic digestion process: a review. *Appl Energy* 240:120–137. <https://doi.org/10.1016/J.APENERGY.2019.01.243>
37. Zieliński M, Zielińska M, Cydzik-Kwiatkowska A et al (2021) Effect of static magnetic field on microbial community during anaerobic digestion. *Biores Technol* 323:124600. <https://doi.org/10.1016/J.BIORTECH.2020.124600>
38. Luo J, Li Y, Li Y et al (2021) Waste-to-energy: cellulase induced waste activated sludge and paper waste co-fermentation for efficient volatile fatty acids production and underlying mechanisms. *Biores Technol* 341:125771. <https://doi.org/10.1016/J.BIORTECH.2021.125771>
39. Park TJ, Ding W, Cheng S et al (2014) Microbial community in microbial fuel cell (MFC) medium and effluent enriched with purple photosynthetic bacterium (*rhodospseudomonas* sp.). *AMB Express* 4:1–8. <https://doi.org/10.1186/S13568-014-0022-2>
40. Albarracín-Arias JA, Yu C-P, Maeda T et al (2021) Microbial community dynamics and electricity generation in MFCs inoculated with POME sludges and pure electrogenic culture. *Int J Hydrogen Energy* 46:36903–36916. <https://doi.org/10.1016/J.IJHYDENE.2021.08.218>
41. Adamberg S, Tomson K, Vija H et al (2014) Degradation of fructans and production of propionic acid by bacteroides thetaiotaomicron are enhanced by the shortage of amino acids. *Front Nutr* 1:1–10. <https://doi.org/10.3389/FNUT.2014.00021>
42. Mateo S, Zamorano-López N, Borrás L et al (2018) Effect of sludge age on microbial consortia developed in MFCs. *J Chem Technol Biotechnol* 93:1290–1299. <https://doi.org/10.1002/JCTB.5488>
43. Li Y, Zhang Y, Kong X et al (2017) Effects of ammonia on propionate degradation and microbial community in digesters using propionate as a sole carbon source. *J Chem Technol Biotechnol* 92:2538–2545. <https://doi.org/10.1002/jctb.5260>
44. Saif I, Salama ES, Usman M et al (2021) Improved digestibility and biogas production from lignocellulosic biomass: biochar addition and microbial response. *Ind Crops Prod* 171:113851. <https://doi.org/10.1016/J.INDCROP.2021.113851>
45. Ma K, Cao Z, Cui Y et al (2021) Effect of magnetite on anaerobic digestion treating saline wastewater: methane production, biomass aggregation and microbial community dynamics. *Biores Technol* 341:125783. <https://doi.org/10.1016/J.BIORTECH.2021.125783>
46. Zhou M, Yang H, Zheng D et al (2019) Methanogenic activity and microbial communities characteristics in dry and wet anaerobic digestion sludges from swine manure. *Biochem Eng J* 152:107390. <https://doi.org/10.1016/J.BEJ.2019.107390>

**Publisher's note** Springer Nature remains neutral with regard to jurisdictional claims in published maps and institutional affiliations.